International Journal on Magnetic Particle Imaging
Vol 9, No 1, Suppl 1, Article ID 2303047, 5 Pages

Infinite Science Publishing

Proceedings Article

Field-swept magnetic particle spectroscopy using a transverse DC field

Yanjun Liu[a,b,c,d] · Xin Feng[c,d,*] · Haoran Zhang[a,b,c,d] · Sijia Liu[c,d,e] · Guanghui Li[a,b,c,d] · Yu An[a,b,c,d] · Hui Hui[c,d,f,*] · Jie Tian[a,b,c,d,e,g,*]

[a]School of Engineering Medicine & School of Biological Science and Medical Engineering, Beihang University, Beijing, 100191, People's Republic of China
[b]Key Laboratory of Big Data-Based Precision Medicine (Beihang University), Ministry of Industry and Information Technology of the People's Republic of China, Beijing, 100191, People's Republic of China
[c]CAS Key Laboratory of Molecular Imaging, Institute of Automation, Chinese Academy of Sciences, Beijing, 100190, People's Republic of China
[d]Beijing Key Laboratory of Molecular Imaging, Beijing, 100190, People's Republic of China
[e]School of Computer Science and Engineering, Southeast University, Nanjing, 210096, China
[f]University of Chinese Academy of Sciences, Beijing, 100080, People's Republic of China
[g]Zhuhai Precision Medical Center, Zhuhai People's Hospital, affiliated with Jinan University, Zhuhai, 519000, China
*Corresponding author, email: xin.feng@ia.ac.cn; hui.hui@ia.ac.cn; tian@ieee.org

Abstract

The transverse magnetization of magnetic nanoparticles (MNPs) induced by a DC field perpendicular to the AC field is of increasing interest in magnetic particle imaging (MPI) and magnetic particle spectroscopy (MPS). It can be used to improve the image quality in MPI and to enhance the sensitivity of MPS without direct feedthrough interference. In this work, we developed a field-swept MPS to observe the response curve of the transverse magnetization by varying the transverse DC field amplitude, and reported a new metric to characterize the nonlinear properties of MNPs, called DCM (the DC field amplitude at the maximum harmonic amplitude). Two commercial MNPs (synomag®-70 and synomag®-50) were investigated. The experimental results show that the DCM is different for the two MNPs and independent of the concentration of MNPs. In addition, the DCM was positively correlated with the viscosity of the sample solvent, which further indicates a correlation with Brownian relaxation.

I. Introduction

Previous study has proposed a static field magnetic particle spectroscopy (sMPS) that uses a pair of permanent magnets generating a uniform static magnetic field perpendicular to the alternating field to induce magnetic nanoparticles (MNPs) to produce a magnetization component along the static field direction, and then records the dynamic magnetization using a receiver coil aligned with the static field [1]. This particular detection approach achieves decoupling of the MNPs signal from the direct feedthrough of the alternating field, which is beneficial to enhance the detection limit of MNPs and is easily extended to current magnetic particle imaging (MPI) systems. [2].

To distinguish from the standard magnetization parallel to the alternating field, we call the magnetization component perpendicular to the alternating field the

transverse magnetization. Recently, transverse magnetization signal has been used to improve the spatial resolution of MPI images in the orthogonal direction of excitation [3], and its ability in improving the sensitivity and spatial resolution of MPI has also been investigated [4]. Previous studies have shown that AC and DC fields with an appropriate amplitude ratio can maximize the harmonic amplitude of specific particles, which is useful for optimizing signal strength [1], [4], but the appropriate field amplitude ratio for different particles may be different, which requires more investigation.

Multi-parametric measurement techniques with frequency sweeping or offset field sweeping are important tools for quantifying the nonlinear magnetization dynamics of MNPs, allowing investigation of specific influencing factors such as viscosity and temperature of the particle environment as well as excitation frequency and excitation field amplitude [5], [6], [7], [8]. Draack et al. proposed a multi-parametric MPS with AC field and DC field in the same direction and analyzed the characteristic changes of the whole spectrum and dynamic magnetization curve of particles with different viscosity in detail [7]. For transverse magnetization, similar techniques need to be developed to investigate the behavior of MNPs in specific sensing or MPI scenarios.

In this study, we develop a field-swept MPS using a transverse static field (DC field) with adjustable amplitude perpendicular to the alternating field (AC field). Several specific even harmonics of the transverse magnetization signal are plotted as functions of the DC field amplitude. Here we focus on the analysis of the relationship between the DC field amplitude at the maximum harmonic amplitude (DCM) and the properties of the MNPs. The experimental results show the specificity of the DCM for different MNPs, demonstrating that the DCM is related to the saturation magnetic moment and relaxation effects of the particles, independent of the number of particles.

II. Methods and Materials

II.I. Theoretical Model

Two mutually orthogonal AC and DC fields are used to excite the particles, the AC field is used to deflect the particles, and the DC field is used to polarize the particles to produce a net magnetization. Here, we only observe the magnetization component along the direction of the DC field, which is called the transverse magnetization M_{T}. Langevin function $\mathscr{L}(\xi)$ is introduced here to describe the nonlinear magnetization of particles, then M_{T} can be written as [1]:

$$M_{\mathrm{T}} = N m_{\mathrm{s}} \mathscr{L}\left(\beta \|\mathbf{H}\|\right) \frac{H_{\mathrm{DC}}}{\|\mathbf{H}\|}, \tag{1}$$

where N is the number of particles per unit volume, m_{s} is the magnetic moment of the particle, β is related to the core diameter, the material and temperature of the particle.

Define DC field H_{DC} in x-direction and AC field H_{AC} in y-direction, then the total applied magnetic field $\mathbf{H}$ can be written as

$$\mathbf{H}(t) = H_{\mathrm{DC}} \mathbf{e}_{\mathbf{x}} + H_{\mathrm{AC}} \cos(\omega_0 t)\, \mathbf{e}_{\mathbf{y}}. \tag{2}$$

Further, substituting the Taylor expansion of $\mathscr{L}(\xi)$ and (2) into (1), we can obtain:

$$\begin{aligned} M_{\mathrm{T}} &= N m_{\mathrm{s}} \left[\frac{\beta \|\mathbf{H}\|}{3} - \frac{\beta^3 \|\mathbf{H}\|^3}{45} + \cdots \right] \frac{H_{\mathrm{DC}}}{\|\mathbf{H}\|} \\ &= N m_{\mathrm{s}} [a_0 - a_2 \cos(2\omega_0 t) + a_4 \cos(4\omega_0 t) \cdots] \\ &= N m_{\mathrm{s}} \sum_{k=0}^{\infty} a_{2k} \cos(2k\omega_0 t), \end{aligned} \tag{3}$$

where $A_{2k} = N m_{\mathrm{s}} a_{2k}$ denotes the amplitude of the $2k$-order harmonic component under adiabatic condition. a_{2k} is a unitless factor related to β and the amplitude of the AC/DC field. Further, considering the dynamic magnetization process in practical measurement, the amplitude of the harmonic components of the transverse magnetization signal with relaxation effect can be described as a nonlinear function:

$$\tilde{A}_{2k} \propto \mathscr{F}\left(H_{\mathrm{DC}}, H_{\mathrm{AC}}, \beta, \tau\right), \tag{4}$$

where τ is the effective relaxation time constant, which is generally a superposition of Brownian and Néel relaxations.

II.II. Spectrometer

The schematic of the experimental spectrometer is shown in Fig. 1(a). The AC field was generated by a Helmholtz coil made by winding 56 turns of Litz wire with 350×0.1 mm strands. The inductance of the AC field coil was optimized by adjusting the number of layers of winding and the number of turns per layer to produce a uniform alternating magnetic field at the highest possible frequency. The optimized single coil has 4 layers of 7 turns each, and the total inductance of the pair of coils is 260 µH, allowing it to generate an alternating magnetic field of 10 mT/μ_0 in the frequency range of 0 to 5 kHz. The excitation frequency used in this study is 2.5 kHz. The DC field is generated by a 22-turn solenoid coil with a resistance of 48 mΩ and adjustable amplitude in the range of 0 to 10 mT/μ_0. The receive coil is 10 mm in diameter and is made of 0.2 mm enameled copper wire evenly wound in 4 layers with a total of 240 turns, aligned with the direction of the DC field. A data acquisition card (DAQ) was used to generate AC and DC signals feed to power amplifiers (AE 7548 and AE 7224, AE Techron, USA). Two current probes (DS50UB-10V, DANISENSE, DNK) were used to monitor the current in the AC and DC coils and

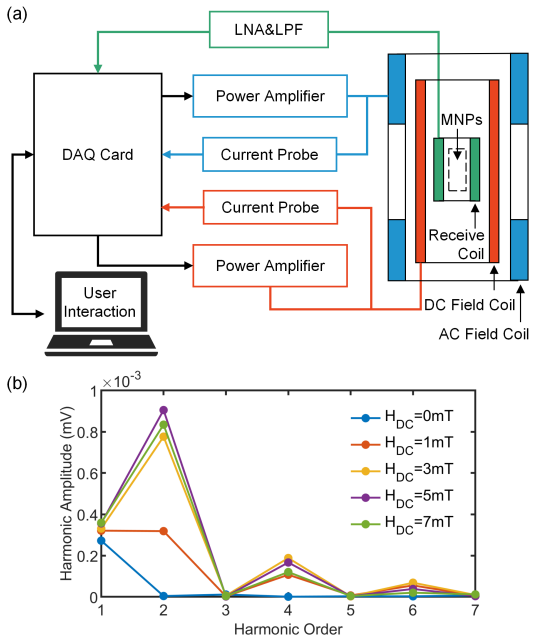

Figure 1: (a) Schematic diagram of the field-swept spectrometer. (b) Fourier spectra with different DC field amplitudes. The sample shown here is synomag-70 with an iron concentration of 1 mg/mL and a glycerol mass fraction of 2%.

feed it back to the DAQ (NI-USB 6356, National Instruments Corporation, USA). The induced voltage signals from the receive coil were transmitted to the low-noise preamplifier (SR560, Stanford Research System, USA) and finally to the DAQ for recording. In this study, SR560 is used as a low-pass filter (LPF) with a cutoff frequency of 30 kHz and an amplification factor of 1. The first to seventh harmonics of the received signal are extracted and analyzed by digital phase-sensitive detection technique, as shown in Fig. 1(b).

II.III. Nanoparticle Samples

Synomag®-D with two hydrodynamic diameters of 70 nm and 50 nm (Micromod GmbH, Germany) were used in this study, which are the multi-core MNPs commonly used in MPI/MPS. The synomag-70 particle used had an amino group on its surface and the stock solution sample had an iron concentration of 6 mg/mL. The synomag-50 particle used had an unmodified dextran surface and the stock solution sample had an iron concentration of 10 mg/mL. Different volume ratios of stock solution and water were mixed to prepare samples with iron concentrations of 0.4, 0.6, 0.8, 1.0 mg/mL in a volume of 200 µL. In addition, synomag-70 was diluted in a mixture of water and glycerin in different proportions (2%, 10%, 20%, 28% and 36%) with a volume of 200 µL and an iron concentration of 1 mg/mL. The viscosity of the five samples was 1.055, 1.311, 1.760, 2.324 and 3.169 mPa·s, respectively.

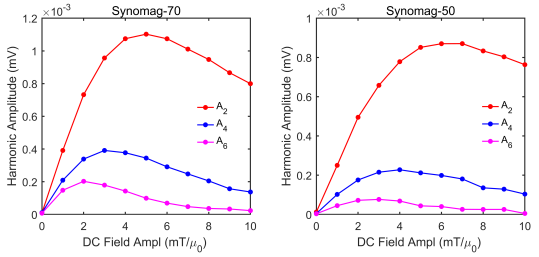

Figure 2: The field-swept harmonic curves (2^{nd}, 4^{th}, and 6^{th} harmonics) of two MNP samples (1.0 mg/mL)

III. Results

Fig. 1(b) shows the Fourier spectra (1st to 7th harmonics) for different DC field amplitudes. When there is no DC field, only the fundamental frequency component is present, which can be attributed to the co-linear magnetization (magnetization in the direction of the AC field) due to the non-perfect orthogonality of the AC field and the receiver coil. When the DC field is present, even harmonics are generated, as demonstrated by (3). As the DC field amplitude increases, the amplitude of the even harmonics shows a non-monotonic variation, and the amplitude of the higher order odd harmonics always remains at a very low level. The fundamental frequency component seems to increase with the DC field amplitude, but it may be related to the linear growth of the background noise, which subsequently needs to be further investigated by a reverse field sweep (e.g., from 10 mT to 0 mT).

Fig. 2 shows the field-swept harmonic curves (2^{nd}, 4^{th}, and 6^{th} harmonics) of two MNP samples. With the increase of H_{DC}, the harmonic amplitude changes nonlinear and reaches a maximum value at a certain DC field amplitude. With the increase of harmonic frequency, DCM is smaller. Note that the DCM values of the different MNPs are significantly different, with the DCM of synomag-70 being significantly smaller than that of synomag-50. The iron concentration of the two MNP samples here is 1 mg/mL, so the difference in DCM is only determined by the nonlinear properties of the particles, such as magnetic moments and relaxation. For the given excitation field parameters in this study, the signal intensity of synomag-70 is greater than that of synomag-50 with the same iron concentration, but the DCM behaves in the opposite way, which further indicates that DCM may be negatively correlated with the effective magnetic moment of MNP.

Fig. 3 shows the 2^{nd} field-swept harmonic curves (top row) and their derivatives $\partial \tilde{A}_2/\partial H_{\mathrm{DC}}$ (bottom row) of MNP samples with different iron concentrations. Although the signal intensity decreases with decreasing concentration, the DCM values does not change significantly. Derivative curves of the same MNPs with different

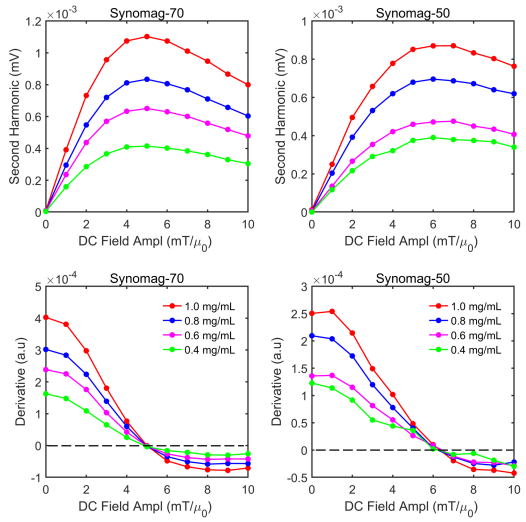

Figure 3: The 2^{nd} field-swept harmonic curves of MNP samples with different concentrations and their derivatives.

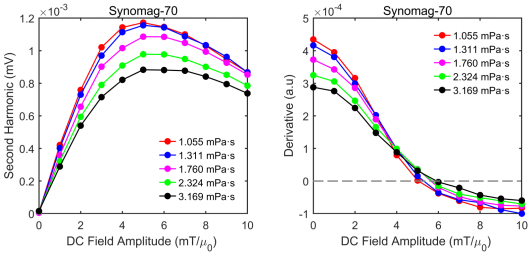

Figure 4: The 2^{nd} field-swept harmonic curves of MNP samples with different viscosities (left) and their derivatives (right).

concentrations all intersect at the zero, which indicated that DCM is specific for MNPs and may be independent of concentration.

Fig. 4 shows the 2^{nd} field-swept harmonic curves (left) and their derivatives (right) of synomag-70 MNP with different viscosities. The experimental results show that the value of DCM increases with the increase of viscosity. Since the Brownian relaxation time is proportional to the viscosity, it can be inferred that DCM may be positively correlated with the Brownian relaxation time of MNPs. It is estimated that the behavior of synomag-50 may be more complicated due to the combined effect of Néel relaxation and Brownian relaxation, which still needs further investigation.

IV. Discussion and Conclusion

In this work, we proposed a field-swept MPS for studying the transverse magnetization response characteristics of MNP. The experimental results show that the DCM is related to the magnetic moment and Brownian relaxation. In the next step we will measure freeze-dried particle samples to investigate the effect of Néel relaxation. The proposed field-swept MPS provides an alternative research tool for multicolor MPI and MNP-based multiparameter sensing.

In addition, the field-swept MPS technically describes a 1D system function along the orthogonal direction of the excitation field [9], [10], [11], which may be useful for constructing more realistic and reliable system function models in the future.

Acknowledgments

This work was supported in part by the National Key Research and Development Program of China under Grant: 2017YFA0700401; the National Natural Science Foundation of China under Grant: 62027901, 81827808, 81930053, 81227901; CAS Youth Innovation Promotion Association under Grant 2018167 and CAS Key Technology Talent Program; Guangdong Key Research and Development Program of China (2021B0101420005); the Project of High-Level Talents Team Introduction in Zhuhai City (Zhuhai HLHPTP201703). The authors would like to acknowledge the instrumental and technical support of multimodal biomedical imaging experimental platform, Institute of Automation, Chinese Academy of Sciences.

Author's statement

Conflict of interest: Authors state no conflict of interest.

References

[1] D. B. Reeves, and J. B. Weaver. Magnetic nanoparticle sensing: decoupling the magnetization from the excitation field, Journal of Physics D-Applied Physics, vol. 47, no. 4, Jan, 2014, 045002.

[2] J. B. Weaver. Perpendicular Magnetic Particle Imaging, pMPI, IEEE Trans. Magn., vol. 51, no. 2, Feb, 2015, 5100404.

[3] M. Graeser, F. Thieben, P. Szwargulski et al. Human-sized magnetic particle imaging for brain applications, Nat. Commun., vol. 10, no. 1, pp. 1936, Apr 26, 2019, 1936.

[4] S. Ota, K. Nishimoto, T. Yamada, and Y. Takemura. Second harmonic response of magnetic nanoparticles under parallel static field and perpendicular oscillating field for magnetic particle imaging, Aip Advances, vol. 10, no. 1, Jan, 2020, 015007.

[5] J. Zhong, W. Liu, Z. Du, P. C. de Morais, Q. Xiang, and Q. Xie. A noninvasive, remote and precise method for temperature and concentration estimation using magnetic nanoparticles, Nanot, vol. 23, no. 7, Feb 24, 2012, 075703.

[6] N. Garraud, R. Dhavalikar, M. Unni, S. Savliwala, C. Rinaldi, and D. P. Arnold. Benchtop magnetic particle relaxometer for detection, characterization and analysis of magnetic nanoparticles, Phys. Med. Biol., vol. 63, no. 17, Sep, 2018, 175016.

[7] S. Draack, N. Lucht, H. Remmer et al. Multiparametric Magnetic Particle Spectroscopy of CoFe2O4 Nanoparticles in Viscous Media, Journal of Physical Chemistry C, vol. 123, no. 11, pp. 6787-6801, Mar 21, 2019.

[8] Z. W. Tay, D. W. Hensley, P. Chandrasekharan, B. Zheng, and S. M. Conolly. Optimization of Drive Parameters for Resolution, Sensitivity and Safety in Magnetic Particle Imaging, IEEE Trans. Med. Imaging, vol. 39, no. 5, pp. 1724-1734, May, 2020.

[9] J. Rahmer, J. Weizenecker, B. Gleich, and J. Borgert. Signal encoding in magnetic particle imaging: properties of the system function, BMC Medical Imaging, vol. 9, no. 1, pp. 1-21, 2009.

[10] P. Szwargulski, and T. Knopp. Influence of the Receive Channel Number on the Spatial Resolution in Magnetic Particle Imaging, Int. J. Magn. Part. Imag., vol. 3, no. 1, Mar 23, 2017, 1703014.

[11] A. von Gladiss, M. Graeser, P. Szwargulski, T. Knopp, and T. M. Buzug. Hybrid system calibration for multidimensional magnetic particle imaging, Phys. Med. Biol., vol. 62, no. 9, pp. 3392-3406, May 7, 2017.

10.18416/ijmpi.2023.2303047